

Supporting Information

2D MXene nanocomposites: Electrochemical and biomedical applications

Marzieh Ramezani Farani¹, Behnam Nourmohammadi Khiarak², Rui Tao³, Zegao Wang³, Sepideh Ahmadi^{4,5}, Mahnaz Hassanpour⁶, Mohammad Rabiee⁷, Mohammad Reza Saeb⁸, Eder C. Lima^{10,*}, Navid Rabiee^{9,11,*}

1. Toxicology and Diseases Group (TDG), Pharmaceutical Sciences Research Center (PSRC), the Institute of Pharmaceutical Sciences (TIPS), Tehran University of Medical Sciences, 1417614411, Tehran, Iran
2. Department of Materials Science and Engineering, Sharif University of Technology, P.O. Box 11365-8639, Tehran, Iran
3. College of Materials Science and Engineering, Sichuan University, Chengdu 610065, China
4. Department of Medical Biotechnology, School of Advanced Technologies in Medicine, Shahid Beheshti University of Medical Sciences, Tehran, Iran
5. Cellular and Molecular Biology Research Center, Shahid Beheshti University of Medical Sciences, Tehran, Iran
6. Department of Chemistry, Institute for Advanced Studies in Basic Sciences (IASBS), Zanjan 45137-66731, Iran
7. Biomaterials Group, Department of Biomedical Engineering, Amirkabir University of Technology, Tehran, Iran
8. Department of Polymer Technology, Faculty of Chemistry, Gdańsk University of Technology, G. Narutowicza 11/12 80-233, Gdańsk, Poland
9. School of Engineering, Macquarie University, Sydney, New South Wales, 2109, Australia
10. Institute of Chemistry, Federal University of Rio Grande Do Sul (UFRGS), Av. Bento Goncalves 9500, Postal Box, 15003, ZIP, 91501-970, Brazil
11. Department of Materials Science and Engineering, Pohang University of Science and Technology (POSTECH), 77 Cheongam-ro, Nam-gu, Pohang, Gyeongbuk, 37673, South Korea

*Corresponding authors: Dr Navid Rabiee (nrabiee94@gmail.com;
navid.rabiee@mq.edu.au) & Prof. Eder C. Lima (profederlima@gmail.com)

S1. SYNTHESIS PROCEDURE

S1.1. Synthesis of MXene

M-X and M-A bond strengths are the most distinctions in MAX phases, which should be carefully considered in the synthesizing process. In fact, the M-A bond is the possible bond to break down rather than the M-X bonds. Therefore, it has been suggested that fabricating carbides and nitrides can be obtained by breaking the M-A weak bonds and removing A layers, which is the most important step in producing MXene phases. On the other hand, it is well-known that the MXene synthesis process takes a long etching time, and, in some cases, the produced structure is not highly durable in practical applications. In this regard, Mo-based MXenes have emerged with some remarkable properties like higher stability and facile and scalable routes to synthesize Mo-MXene. Besides, it requires a short etching time to be synthesized. Therefore, Mo-MXenes are among the major focus among researchers and have been synthesized through etching the related MAX phase.

In 2020, Lim et al. ¹ effectively achieved Mo-based MXene through a simple and scalable two steps approach of in situ sulfidations of Mo_2CT_x MXenes to produce a hybrid $\text{Mo}_2\text{CT}_x/2\text{H-MoS}_2$ via a simple and routine synthesis procedure (**Figure S1**) ². Numerous compositions of Mo-based MXenes have been reported, such as $\text{Mo}_2\text{TiC}_2\text{T}_x$, $\text{Mo}_2\text{Ti}_2\text{C}_3\text{T}_x$, $\text{Mo}_2\text{ScC}_2\text{T}_x$, and $\text{Mo}_4\text{VC}_4\text{T}_x$ ^{3, 4}. The most common method can be associated with the HF etching process. $\text{Mo}_4\text{VC}_4\text{T}_x$ can be considered the state-of-the-art material since it has been derived from the most recently explored Mo_4VAIC_4 . The M atom layers have been expanded to five atom layers ⁵. In another interesting work by Joshi et al. (Joshi et al. 2017), they considered a two-step approach to synthesizing Mo-MXene. In the first step, a chemical vapour deposition (CVD) was used to fabricate MoO_3 phases on a fluorinated tin oxide substrate. The heating filaments of Mo do this step under O_2 gas flow. Afterwards, the produced MoO_3 from the CVD route was annealed under an ammonia atmosphere; this has eventuated in MoN phase formation as a result of MoO_3 phase transformation.

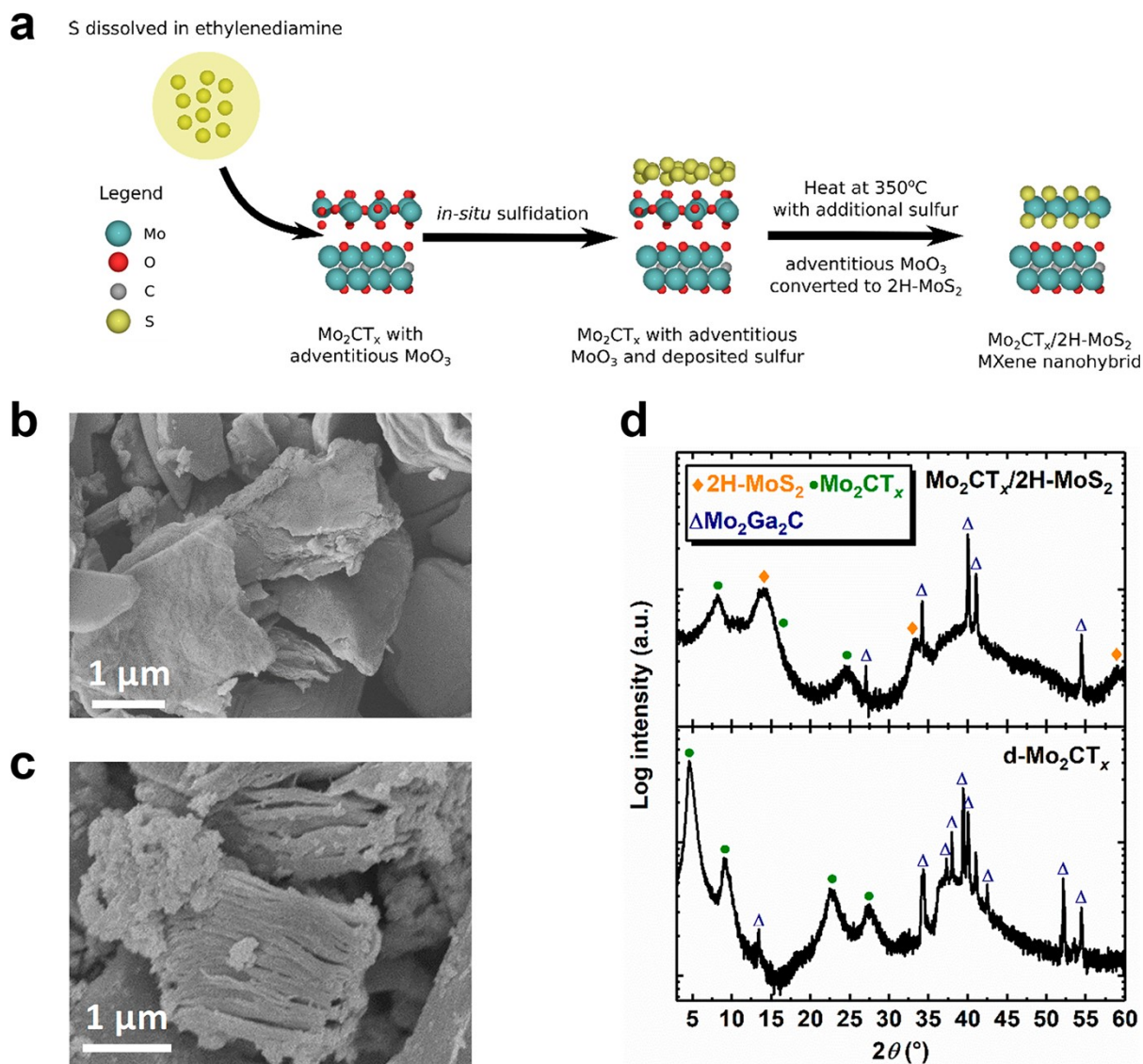


Figure S1. (a) Schematic of producing Mo₂CT_x/2H-MoS₂ nanohybrid. SEM of (b) d-Mo₂CT_x, (c) Mo₂CT_x/2H-MoS₂. (d) XRD spectra of d-Mo₂CT_x before sulfidation and Mo₂CT_x/2H-MoS₂ after sulfidation. Mo₂Ga₂C peaks mention the Mo₂Ga₂C precursor retained during synthesis¹.

Another important component that has attracted great attention in MXene is Vanadium (V). V-based MXenes were synthesized in 2012 by Naguib et al.⁶ that gained much attention in the years after that due to their functional, significant, and extra-ordinary layer-by-layer structures (**Figure S2**), and afterwards, V-containing MXenes have appeared extensively⁷. One of the most conspicuous behaviours of V-based MXene is their high capacitance than well-known Ti₃C₂T_x. Hence, it has been highly significant for further study and its potential application in electrochemical energy storage and conversion^{8, 9}. Until

now, numerous methods have been proposed to synthesize V-based MXene materials. In this regard, Naguib et al.⁷ have fabricated V_2CT_x MXene from V_2AlC by etching out the Al layer by utilizing an HF solution. They could successfully synthesize V-based MXene and develop them. In this route, they found that a bit of long-time etching out is required compared to conventional $Ti_3C_2T_x$ MXene.

Moreover, Guan et al.¹⁰ have employed a mixed etching solution composed of HF and HCl to fabricate the V_2CT_x MXene phase. Inspired by that work, Liu et al.¹¹ also employed a mixed etchant solution of NaF + HCl. The clearest difference was in etching time, which was about 72 hours. Through approaches, they could have obtained fine exfoliated structures with single layers.

A new method has recently emerged, termed as molten $ZnCl_2$ etching process. In this route, since a Lewis acidic solution composed of molten $ZnCl_2$ is being used, a very short time is necessary to complete the fabrication process, almost 5 hours. Therefore, this synthesizing approach is faster than the conventional HF etchant-based method. In addition to the aforementioned works, Wang et al.¹² achieved $V_4C_3T_x$ by etching the V_4AlC_3 by employing an HF etching solution. The HF etching route is the most common way to produce V-based MXenes, and fluoric salt + HCl etching solution is still among the most generally accepted approaches to obtaining V-based MXene. However, the long synthesis time and severely toxic solution are the enormous difficulties requiring more user-friendly approaches for synthesizing MXenes^{13, 14}.

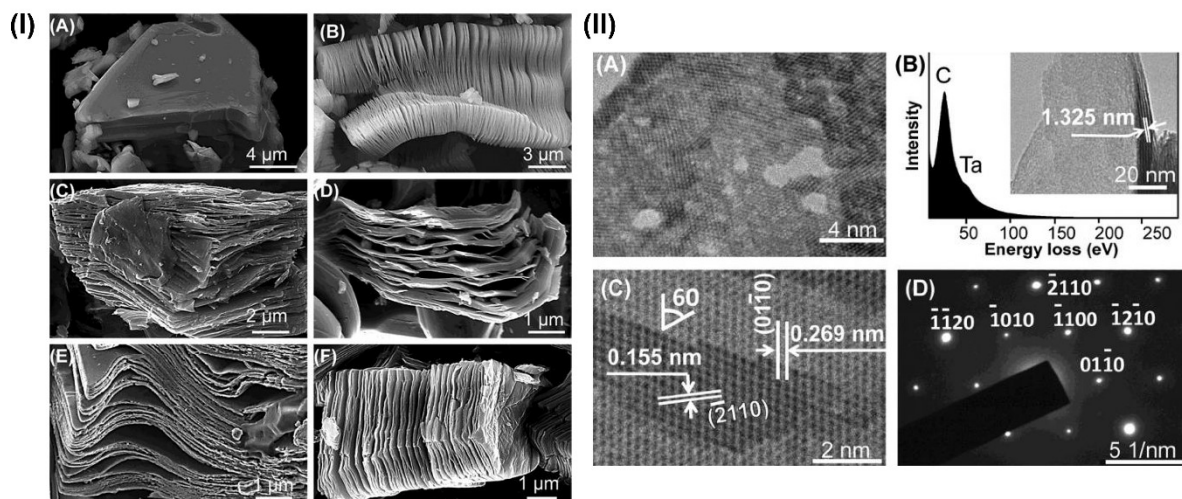


Figure S2. (I) SEM of (A) Ti_3AlC_2 particle before treatment, (B) Ti_3AlC_2 after HF treatment, (C) Ti_2AlC after HF treatment, (D) Ta_4AlC_3 after HF treatment, (E) $TiNbAlC$ after HF treatment, (F) Ti_3AlCN after HF treatment. (II) Schematic of electron microscopy of Ta_4AlC_3 after HF treatment (A) TEM, (B) EELS, (C) HRTEM of MXene, (D) SAED ⁶.

Niobium-based MXenes are another type that has attracted great interest after their first discovery of it in 2012 by Khazaei et al. ¹⁵. It was hypothesized to have higher stability due to Nb-based structures. Afterwards, additional evaluations demonstrated that Nb-based MXenes possess the high catalytic activity and biocompatibility ^{8, 16-18}. Generally, exfoliated layers of Nb_2CT_x MXene structures would be obtained through three various etching approaches, including the conventional HF etching route, $LiF+HCl$ etching way, and hydrothermal way.

Investigations have shown that the HF etching method possesses higher quality among these three ways with higher effective exfoliation than the other methods ^{19, 20}. However, although $LiF+HCl$ mixed etchant has been confirmed to be a strong solution for synthesizing $T_3C_2T_x$ structures, it is not a good candidate for synthesizing Nb_2CT_x . This can be related to the strict bonding properties of Nb-Al to overcome. The hydrothermal route for Nb-based MXene fabrication has been discovered by Peng et al. This route, a combination of $NaBF_4$ and HCl, is used as an etchant solution.

Among various types of MXenes that are made of Nb can be mentioned to $TiNbCT_x$, which was developed by Naguib et al. ⁶, $(Nb_{0.8}T_{0.2})_4C_3T_x$ and $(Nb_{0.8}Zr_{0.2})_4C_3T_x$ structures by

Yang et al.,²¹ and a novel structure composed of $\text{Nb}_{3.5}\text{W}_{0.5}\text{C}_3\text{T}_x$ by Cai et al.,²². Interestingly, all of these MXene-based nanostructures could be able to characterize easily by XPS spectra, and in the case of $\text{Nb}_{3.5}\text{W}_{0.5}\text{C}_3\text{T}_x$, it was successfully characterized by XPS (**Figure S3**) (however, the difference between some bands are little, but in this field, it would be so applicable and precise than XRD and FTIR). Therefore, it would be more sustainable, affordable, and fast just to prepare a full library of XPS of these MXene-based nanostructures and compare them to each other.

Normally, all the aforementioned MXenes require a long-time synthesizing process; for example, fabricating $(\text{Nb}_{0.8}\text{Zr}_{0.2})_4\text{C}_3\text{T}_x$ demands a long hour of 168 to be etched out and exfoliated. With bearing in mind the aforementioned discussions, in the following sections, we will delve into some cogent explanations of synthesizing routes to deeply understand the effect and importance of the fabrication method.

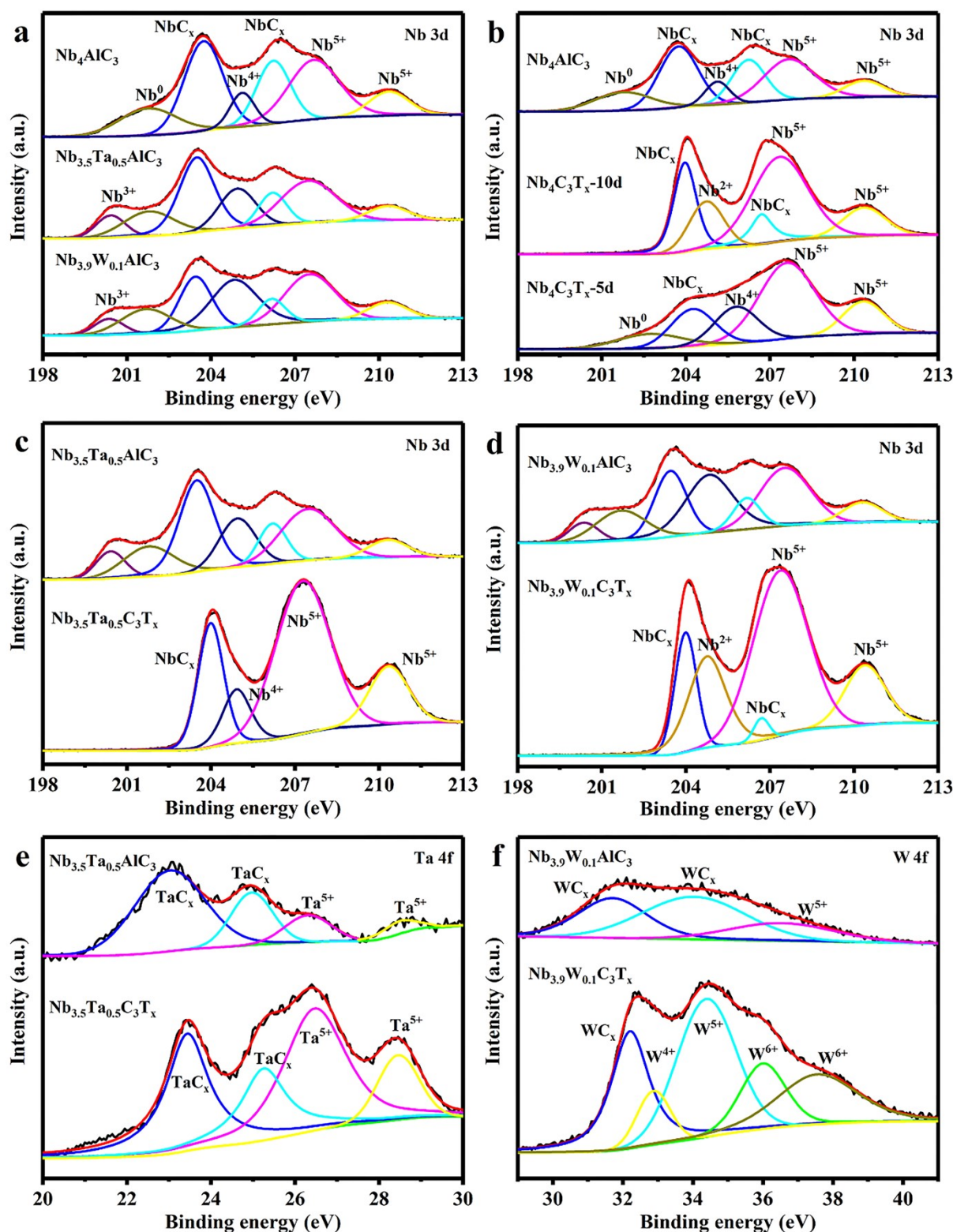


Figure S3. XPS spectra in order to (a) Nb 3d of Nb_4AlC_3 , $\text{Nb}_{3.5}\text{Ta}_{0.5}\text{AlC}_3$ and $\text{Nb}_{3.9}\text{W}_{0.1}\text{AlC}_3$ MAX ceramics, (b) Nb 3d of Nb_4AlC_3 , N10 and N5, (c) Nb 3d of $\text{Nb}_{3.5}\text{Ta}_{0.5}\text{AlC}_3$ and T5, (d) Nb 3d of $\text{Nb}_{3.9}\text{W}_{0.1}\text{AlC}_3$ and W5, (e) Ta 4f of $\text{Nb}_{3.5}\text{Ta}_{0.5}\text{AlC}_3$ and T5, (f) W 4f of $\text{Nb}_{3.9}\text{W}_{0.1}\text{AlC}_3$ and W5 samples ²².

S1.2. Synthesis of MXene from MAX phase

Another strategy for MXene fabrication is out of the plane chemically ordered MAX phases (denoted as o-MAX) technique which has received great interest in research to synthesize ordered MXenes. The first o-MAX phase was synthesized in 2014 by Liu and co-workers²³. For the first time, Liu and co-workers synthesized quaternary MXene structures, which they fabricated a chemically ordered $\text{Cr}_2\text{TiAlC}_2$ ²³. In this type of MXene structure, Ti layers are positioned between Cr and carbide layers.

Therefore, exploring ordered MXenes phases obtained new insight into these new 2D materials' family. This discovery was followed by the synthesis of $\text{Mo}_2\text{ScC}_2\text{T}_x$ by Meshkian and co-workers²⁴, $\text{Ti}_2\text{ZrAlC}_2$ discovery by Tunca and co-workers²⁵, and $\text{Mo}_2\text{TiAlC}_2$ discovery by Anasori and co-workers²⁶ and so many other discoveries in this regard. Moreover, Meshkian and co-workers demonstrated a theoretical prediction besides experimental indication of ordered MXene phases^{24, 27}.

In that work, they synthesized the first Scandium-containing MXene phase, which the synthesized MXene is composed of chemically ordered transition metals, and presented their synthesized structure as $\text{Mo}_2\text{ScC}_2\text{T}_x$. In fact, in that work, Meshkian and co-workers, with theoretical and experimental evidence, demonstrated the existence of quaternary MXene phases with chemical order. Furthermore, they showed a sandwich structure of Mo, Sc, and C in which Sc layers have been formed between Mo-C layers. Generally, high-resolution transmission electron microscope (HRTEM), scanning electron microscope (SEM), and specifically high-resolution STEM (**Figure S4**) demonstrated that the chemical order in the MXene structure results in high phase stability than the regular MXene phases, in which they have revealed that chemically ordered $\text{Mo}_2\text{ScC}_2\text{T}_x$ is more stable than Mo_3AlC_2 and Sc_3AlC_2 ²⁴. Furthermore, it has been shown that MXenes phases with higher "n" require strong etching conditions; therefore, although $\text{Mo}_2\text{ScC}_2\text{T}_x$ and Mo_3AlC_2 , and Sc_3AlC_2 are isostructural, due to their various M layers make them show remarkably various electronic properties. Besides, $\text{Mo}_2\text{ScC}_2\text{T}_x$ displayed semiconductor-like transport behaviour, while Mo_3AlC_2 and Sc_3AlC_2 exhibit metallic properties.

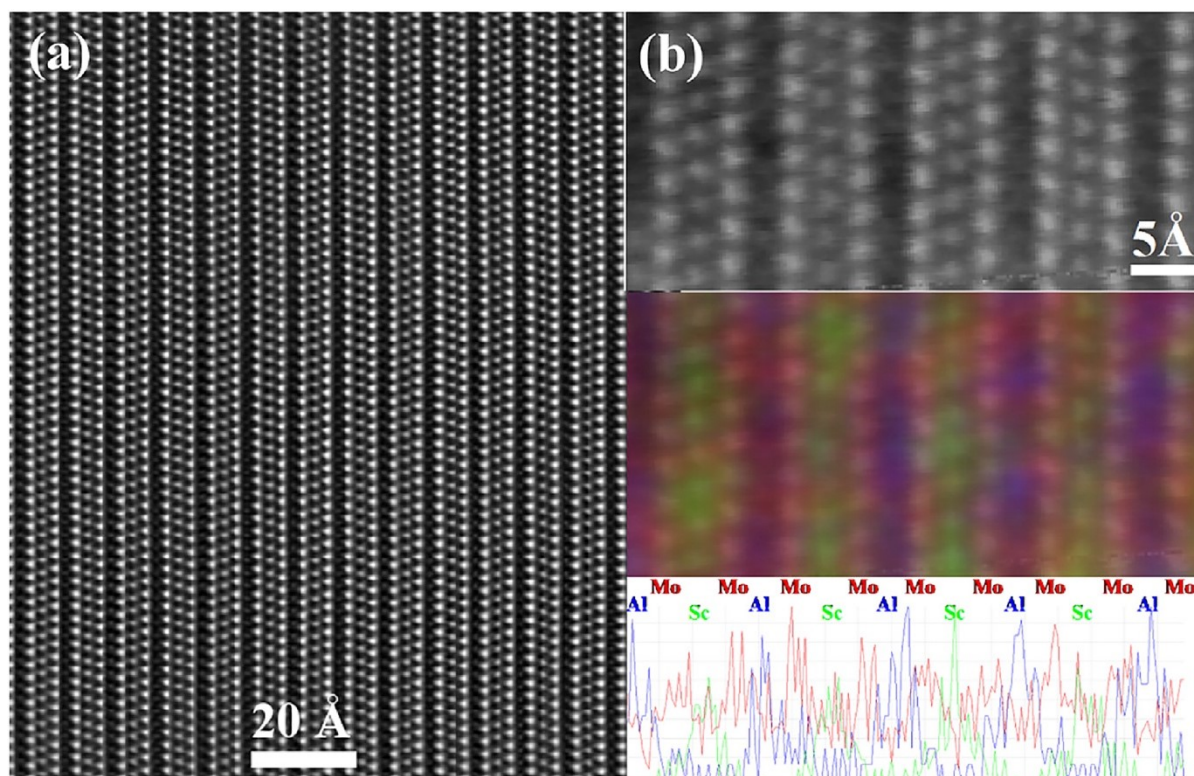
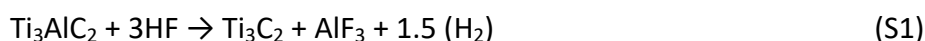


Figure S4. The experimental evidence in Meshkian and co-workers, (a) HR(S) TEM photo displays the laminated structure of the MAX phase. (b) EDX elemental map to Mo, Sc, and Al shows the distribution of the embedded elements in the sample (Ref. ²⁴).

S1.3. Synthesis of MXene via a wet chemical method

Several methods can fabricate MXenes ²⁸⁻³⁰. In the initial synthetic route for MXenes, fluoric acid (HF) was used, and sonication in methanol or isopropyl was used to exfoliate layers. HF was used along with constant agitation in this route, which resulted in a good-quality multilayer structure. The chemical reaction in this method can be explained as below, which was proposed in the initial study:



The equations (S1-S3) demonstrate the exact process of MXenes synthesis. In Eq.S1, as can be seen, the removal of aluminium atoms happens (remove of "A" layers from MAX phase), and in Eq.2, 3, the surface terminations in MXenes structure created (in this case,

hydroxyl and fluorine atoms form surface terminations). In some cases reported in the literature, some oxygen terminations are also detected in MXenes structure³¹⁻³³. It also can be said that the Ti-Al bonds are replaced by Ti-OH, Ti-F, and Ti-O bonds. Since now, most of the experimentally fabricated MXenes demonstrate -O, -F, and -OH terminations. This has resulted from their higher thermodynamic durability compared to their pristine counterparts.

Hence, it is obvious that more research must be done to determine the most stable functionalization groups and the method to form a single functional group. As shown above about the synthetic route for MXenes, through the rational choice of proper elements, solvents, synthesis method, and chemical reaction parameter controlling during synthesizing, different usage of transition metals would affect MXene properties, and through that one can successfully synthesis excellent materials toward a wide range of usage. To point out, employing various transition metals and variable terminations on the surface could offer excellent electrochemical activity (for the electrochemical process such as water splitting, supercapacitors, CO₂ conversion, etc.). Moreover, these materials' electronic and structural properties can be controlled, which determines the electrochemical capability by increasing accessible active sites, energy storage efficiency, etc. In this regard, scientists have outlined some fabulous synthetic strategies¹³.

Many factors can influence MXenes during synthesis, such as the sonication process (time and temperature), etching solution and its temperature, MAX phase quality, composition and particle size, intercalation agent, etc. To shed light on this issue, Naguib et al.³⁴ experimentally demonstrated that higher M atom numbers require more time or higher acid concentration to synthesize an MXene.

They conclude that an MXene structure like the M₄AX₃ phase needs harsher etching conditions than regular MXene phases such as M₃AX₂ or M₂AX. Therefore, much research has focused on increasing MXene intercalation efficiency. The freeze-drying technique is among the suitable processes to control the interlayer distances and prevent the restacking of MXene nanosheets which could provide the potential for practical applications.

Fundamentally, strong porous structures can be formed if tough interaction exists between 2D nanosheets. Bao and co-workers have synthesized highly active and high--

surface materials made of MXene by utilizing the freeze-drying technique. The idea was a nest inside the hydrogen-bonding interaction and weak van der Waal's force among various layers of MXene, which has resulted in a high accessible surface area material³⁵⁻³⁷. In this regard, the self-discharge behaviour of different forms of MXenes was investigated by scientists and showed that each step of the synthesis and fabrication process is important for the final application.

For the self-discharge and energy applications, even the annealing process and removal of water from the content could lead to a significant effect on the morphology of the MXene (**Figure S5**), and followed by that, the ability of the nanomaterial to absorb/adsorb the ion/small molecules and interesting changes to the migrations of different cations/anions and then considerable alterations to the energy applications³⁸. Bao et al. demonstrated that the freeze-drying technique could prevent the restacking of MXene nanosheets due to weak van der Waals forces. Ti₃AlC₂ powders were etched with HF solvent to remove aluminium (Al) in this work. Then it was followed by washing and stirring the etched powder in chloroform solvent.

Afterwards, the freeze-drying process helped remove the remaining water and chloroform molecules from the previous process; as a result, the interlayer space between monolayers of intercalated Ti₃C₂T_x enlarged. In this case, it should be highlighted that the enlarged spaces between MXene layers can be associated with the solidification and condensation of water molecules during the freeze-drying process. This phenomenon will eliminate the adverse impact of van der Waals forces between layers and contribute to the more stable and excellent porous structure of MXene (**Figure S6**)³⁵.

Since water molecules function as pore creation and spacers, they have influentially prevented the restacking problem in intercalated MXene (Ti₃C₂T_x), which has eventuated in high accessible surface area that is highly important for practical applications such as energy storage area or biomedical applications. A vacuum freeze-drying process can also prepare a porous MXene structure by employing the solvent as a template. Although the positive point of using the vacuum freeze-drying technique is to hinder the restacking phenomenon of MXene layers, it is known that layered materials with the distance between their layers would provide good accessibility for ion diffusion from the solution that is in contact. In

turn, this can enhance the capacitance behaviour of the material. Besides, the open structures of MXenes can be controlled in a vacuum freeze-drying process by changing the freeze-drying parameters³⁹.

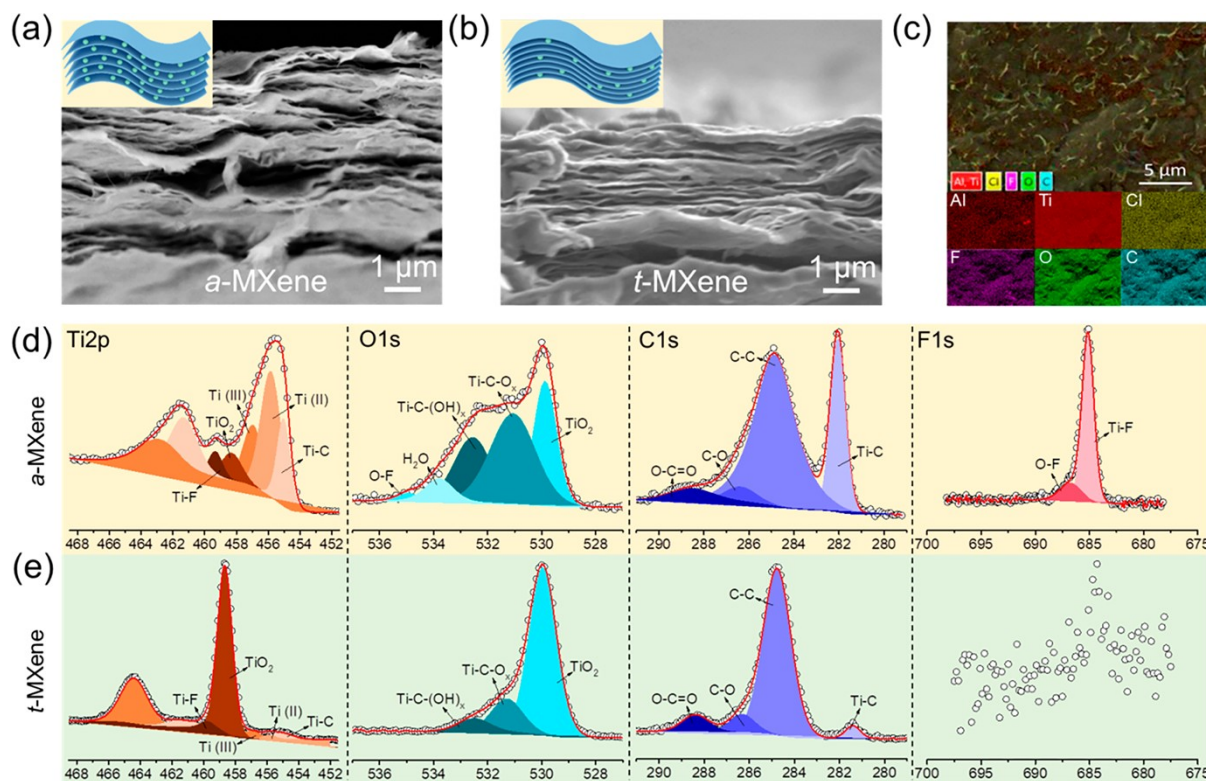


Figure S5. Morphology evolution of *a*-MXene and *t*-MXene films. (a) *a*-MXene and (b) *t*-MXene films. (c) Energy-dispersive spectroscopy mapping of *t*-MXene films. X-ray photoelectron spectra of the (d) *a*-MXene and (e) *t*-MXene films. Reprinted from Ref³⁸.

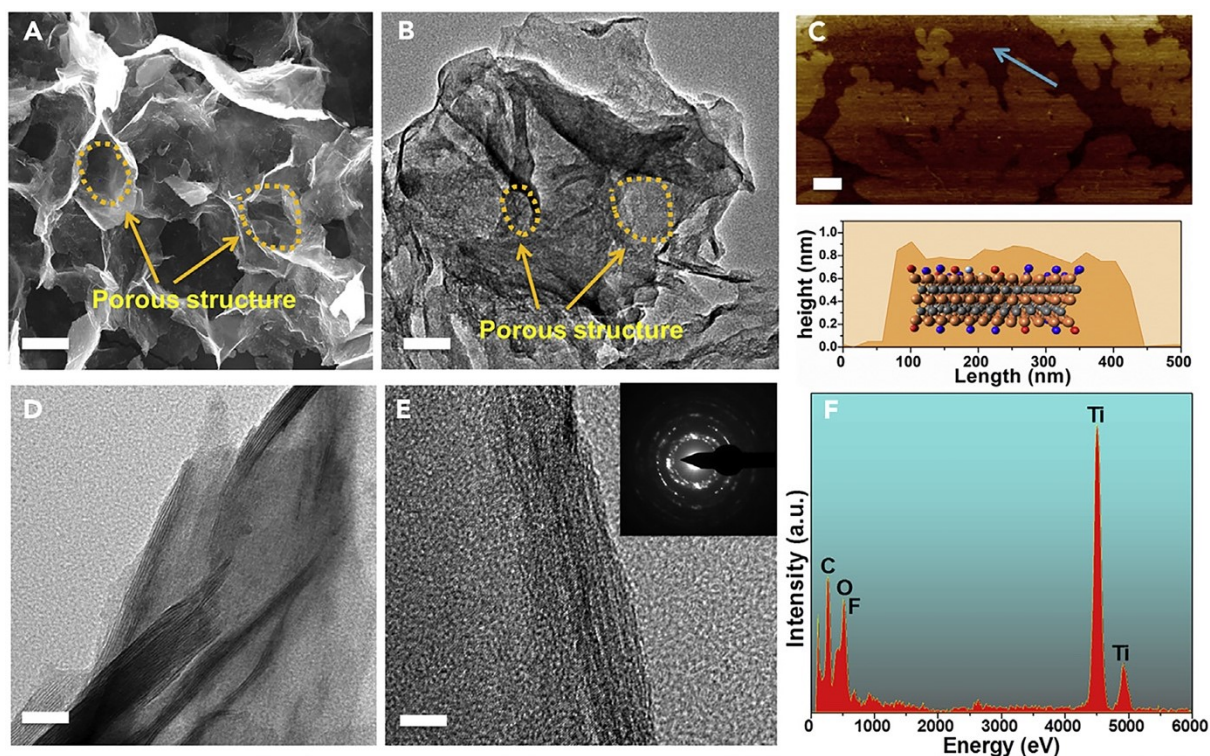


Figure S6. Structural characterization of fabricated porous $\text{Ti}_3\text{C}_2\text{T}_x$ by Bao et al. through freeze-drying technique. (A–G) FESEM (A), HRTEM (B and D), AFM image and thickness profiles laterally the arrow (C), SAED (E), TEM-EDS spectrum (F), images of porous $\text{Ti}_3\text{C}_2\text{T}_x$ architectures. Scale bars are as follows, 200 nm (A), 200 nm (B), 100 nm (C), 20 nm (D), and 5 nm (E). Reprinted from Ref ³⁵

S1.4. Synthesis of MXene via spray drying

Another interesting process to synthesize MXene compounds is spray drying. Spray drying is a way to synthesize porous nanomaterials by capillary force assistance and self-assembly. Xiu and co-workers ⁴⁰ have worked on fabricating MXene phases through the spray drying technique. They firstly reported high-performance MXene phases by facile spray drying route to construct the magnetized MXene/ Fe_3O_4 structure. The prepared MXene/ Fe_3O_4 composites improved absorption activity and broadened influential bandwidth at a thinner thickness. In this work, as shown in **Figure S7**, MXene structures were first synthesized by ultra-sonication aerosol spray drying of MXene suspension. Ti_3C_2 MXene nanosheets were first selectively etched Al layers in Ti_3AlC_2 MAX phase in etchant solution composed of LiF/HCl mixture.

This process was followed by ultra-sonication intercalation; it should note that an Ar-protected atmosphere was used to minimize oxidation. Finally, the MXene suspension is nebulized by ultra-sonication to create aerosol droplets. The prepared droplets are sprayed into a furnace at a high temperature (e.g., 600 °C) to remove solvent since the average size of droplets are few micrometres, or in some cases, nanometer; as soon as these droplets enter the furnace, they easily can be evaporated upon heating in a furnace. Therefore, the obtained materials will be reshaped into a 3D architecture with isotropic compression and assembly of MXene nanosheets due to the inward capillary force, especially after full evaporation of the initial solvent. The synthesized route through spray drying has shown excellent capabilities; the results have exhibited that the obtained porous structure prevents the restacking phenomenon in MXene nanosheets, thereby improving the accessible active sites and improving the prepared 3D porous architecture efficiency kinetically favourable framework for further applications.

As Xiu and co-workers reported in their work, the structure and electronic and other important features of prepared MXene through spray drying can be tuned just by controlling the properties of suspension precursors, which affects the droplets particle size and durability and surface features of ultrasonic formed aerosol droplets. To put into a more vivid picture, employing an appropriate amount of surfactant (e.g., polyvinylpyrrolidone, PVP, and others), which can help ameliorate the surface tension and keep the initial morphology of the aerosol droplets during drying in the furnace^{41,42}. Thus, one can tune the final structure of MXene. In order to control the average size of the MXene structures, variation in the initial concentration of MXene suspension could help control the obtained MXene architecture from 0.5 to 3.5 micrometre. In addition, it is worth noting that in the spray drying process by simply adding metal salts (such as metal phosphide (CoP, NiP), metal oxide (SnO₂, Co₃O₄), perovskite-type metal oxide (MnTiO₃), noble metals (Pt, Ag, Ru, Ir)) into MXene suspension can provide the ability to successfully synthesize a new type of materials with different potentials in real applications while maintaining MXene structure^{36, 43, 44}.

Also, there are some practical and innovative ways to categorize different types of MXenes based on their secondary materials, processing methods as well as their ultimate applications (**Figure S8**); therefore, by this method, it would be possible to increase the

range of new synthetic MXenes for different types of applications through improving/customizing their physicochemical properties. Furthermore, as can be seen, this process is among the favourite methods for fabricating new porous MXene-based composite or hybrid materials for high advanced applications ³⁶.

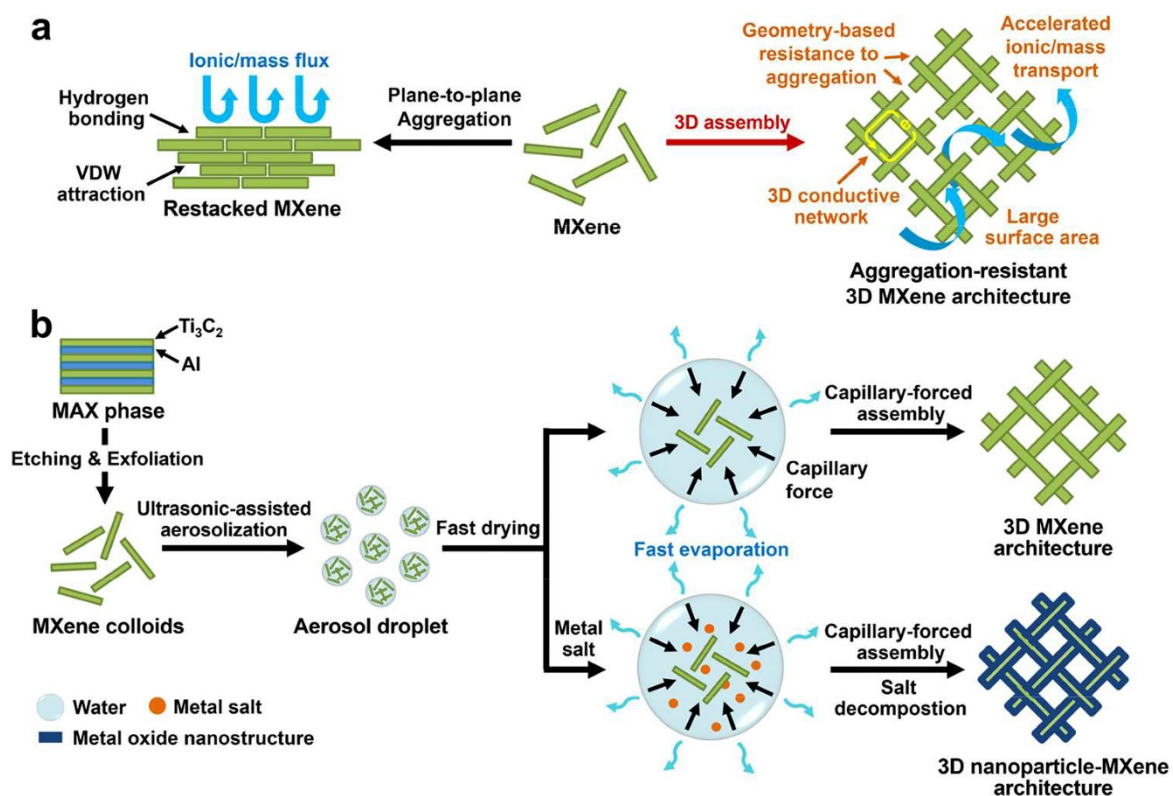


Figure S7. The schematic representation of the process that Xiu and co-workers have done Reprinted from ⁴⁰ (a) visually demonstrated the advantages of layered and spaced structure of 3D MXene, (b) Capillary-forced assembly of MXene to 3D architecture, and corresponding formed composite materials through the spray drying the aerosol droplet of MXene-containing colloids.

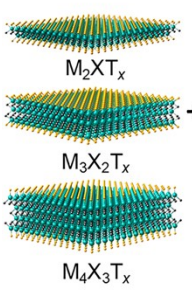
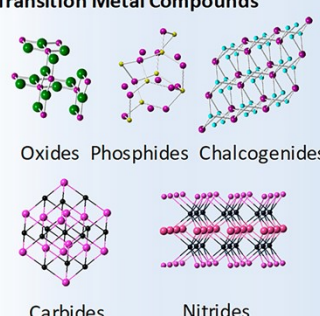
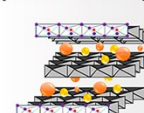
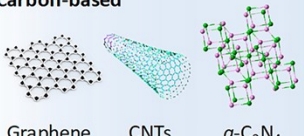
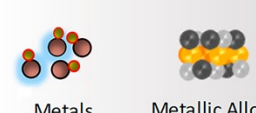
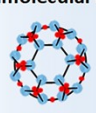
	Secondary Materials	Processing method	Applications
MXenes  $M_2X_2T_x$ $M_3X_2T_x$ $M_4X_3T_x$	Transition Metal Compounds  Oxides Phosphides Chalcogenides Carbides Nitrides	<i>In situ</i> oxidation/sulfidation Hydro/solvothermal synthesis Solution processing Electrostatic self-assembly Electrodeposition Dropcasting	Water splitting: HER/OER Metal-air battery: OER/ORR Metal-S battery: S cathode CO ₂ RR, N ₂ RR
	Layered Double Hydroxides 	Hydro/solvothermal synthesis Electrostatic self-assembly	Water splitting: HER/OER Metal-air battery: OER CO ₂ RR
	Carbon-based  Graphene CNTs <i>g</i> -C ₃ N ₄	Solution processing Electrostatic self-assembly Physical deposition (CVD, ALD)	Water splitting: OER Metal-air battery: OER/ORR Metal-S battery: S cathode CO ₂ RR, N ₂ RR
	Element/ Multi-element  Metals Metallic Alloys	Electrostatic self-assembly Solution processing (self-reduction stabilization)	Water splitting: HER/OER Metal-air battery: OER/ORR CO ₂ RR, N ₂ RR
	Supramolecular Structures  MOFs	Solution processing Electrostatic self-assembly	Water splitting: OER CO ₂ RR

Figure S8. Different types of MXene ($M_2X_2T_x$, $M_3X_2T_x$, and $M_4X_3T_x$) are combined with secondary materials to procedure MXene hybrids. In order to make the MXene hybrids, Communal processing approaches are also listed. Reprinted from ³⁶.

S1.5. Synthesis of MXene via a sacrificial hard-template technique

Another important method to produce an MXene structure is a sacrificial hard-template technique. This process depends on template surfaces, and the template used is eliminated. To shed light on this issue, Zhu and co-workers have synthesized a

supercapacitors electrode from MXene by employing a hard-template strategy⁴⁵. In that work, intercalated MXene nanosheets (Ti_3AlC_2) were first produced using LiF/HCl as an etchant. It should be highlighted that using LiF/HCl instead of HF has some advantages^{14, 46}. Although LiF/HCl produces HF in situ by the following reaction, it has other benefits to be used.



LiF/HCl is a less destructive solvent, needs less sonication time, and outcome efficiency is higher than HF, where more than 70% of the nanosheets have mono-bilayers. As a result, defects and vacancies will be lower than in HF, and the flexibility and ability to reshape will be highly likely than using HF solvent. In fact, in LiF/HCl solvent, a high intercalation yield can be obtained, and since no intercalation agents were used in the process, a better and more flexible MXene will be obtained^{18, 19}. The resulting MXene nanosheets in Zhu and co-workers' work were obtained by centrifuge steps⁴⁵.

The provided MXene nanosheets were used to reshape and prepare other MXene-based materials. The prepared MXene collided and dispersed in MgO (as template), and the obtained suspension was stirred to gain a well-mixed solution. In order to remove the MgO template, during the filtration process, acetic acid was used, and it has gradually added to eliminate the MgO template. Finally, a vacuum filtration process was applied to convert the obtained materials into a free-standing 3D structure. The obtained 3D structure demonstrated spongy-like architecture (**Figure S9**)⁴⁵. A disordered surface can be associated with water molecules' de-intercalation during thermal treatment, which was trapped between MXene layers.

The X-ray diffraction patterns confirmed the self-assembled structure as an interconnected network by a pore-forming process. Among the most interesting properties that have been obtained in this work can be ascribed to its metallic conductivity resulting from good contacts and interaction in MXene networks. In addition, the pore size can be controlled by employing MgO with various pore sizes and diameters, which is important for practical applications.

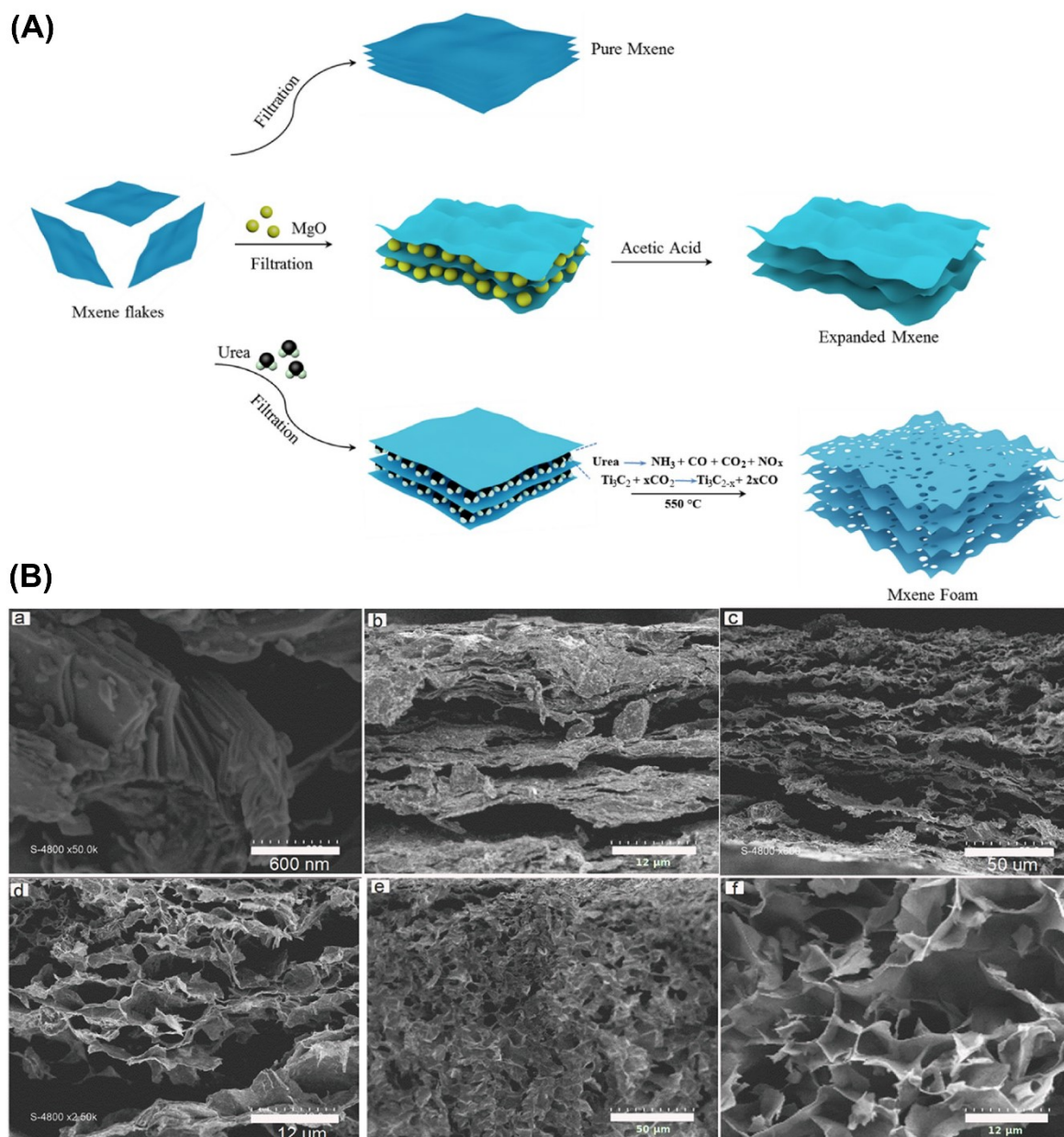


Figure S9. (a) Schematic representation of assortments of MXenes structures after exfoliation (top), MXene after restacking in the existence of MgO npS (middle), and MXene foam from thermal treatment in the existence of urea (bottom), Side visions from SEM of Ti_3AlC_2 MAX phase (b), $\text{Ti}_3\text{C}_2\text{T}_x$ -MXene (c), $\text{Ti}_3\text{C}_2\text{T}_x$ -MXene (d, e) and $\text{Ti}_3\text{C}_2\text{T}_x$ -Mxene foam (f, j). Reprinted from ⁴⁵

References

1. K. R. G. Lim, A. D. Handoko, L. R. Johnson, X. Meng, M. Lin, G. S. Subramanian, B. Anasori, Y. Gogotsi, A. Vojvodic and Z. W. Seh, 2H-MoS(2) on Mo(2)CT(x) MXene nanohybrid for efficient and durable electrocatalytic hydrogen evolution, *ACS Nano*, 2020, **14**, 16140-16155.
2. Z.-X. Cai, X.-H. Song, Y.-Y. Chen, Y.-R. Wang and X. Chen, 3D nitrogen-doped graphene aerogel: A low-cost, facile prepared direct electrode for H₂O₂ sensing, *Sens. Actuators B Chem.*, 2016, **222**, 567-573.
3. B. Anasori, Y. Xie, M. Beidaghi, J. Lu, B. C. Hosler, L. Hultman, P. R. Kent, Y. Gogotsi and M. W. Barsoum, Two-dimensional, ordered, double transition metals carbides (MXenes), *ACS Nano*, 2015, **9**, 9507-9516.
4. L. Zhao and B. Li, Synthesis and recent applications of MXenes with Mo, V or Nb transition metals: a review, *Tungsten*, 2020, 1-18.
5. G. Deysler, C. E. Shuck, K. Hantanasirisakul, N. C. Frey, A. C. Foucher, K. Maleski, A. Sarycheva, V. B. Shenoy, E. A. Stach and B. Anasori, Synthesis of Mo₄VAIC₄ MAX phase and two-dimensional Mo₄VC₄ MXene with five atomic layers of transition metals, *ACS Nano*, 2019, **14**, 204-217.
6. M. Naguib, O. Mashtalir, J. Carle, V. Presser, J. Lu, L. Hultman, Y. Gogotsi and M. W. Barsoum, Two-dimensional transition metal carbides, *ACS Nano*, 2012, **6**, 1322-1331.
7. M. Naguib, J. Halim, J. Lu, K. M. Cook, L. Hultman, Y. Gogotsi and M. W. Barsoum, New two-dimensional niobium and vanadium carbides as promising materials for Li-ion batteries, *J. Am. Chem. Soc.*, 2013, **135**, 15966-15969.
8. B. N. Khiarak, A. Asaadi Zahraei, K. Nazarzade, H. R. Akbari Hasanjani and MohammadzadehHurieh, Shape-controlled synthesis of thorn-like 1D phosphorized Co supported by Ni foam electrocatalysts for overall water splitting, *Journal of Materials Science: Materials in Electronics*, 2021.
9. A. Saadati, B. N. Khiarak, A. A. Zahraei, A. Nourbakhsh and H. Mohammadzadeh, Electrochemical characterization of electrophoretically deposited hydroxyapatite/chitosan/graphene oxide composite coating on Mg substrate, *Surf. Interfaces* 2021, **25**, 101290.
10. Y. Guan, S. Jiang, Y. Cong, J. Wang, Z. Dong, Q. Zhang, G. Yuan, Y. Li and X. Li, A hydrofluoric acid-free synthesis of 2D vanadium carbide (V₂C) MXene for supercapacitor electrodes, *2D Materials*, 2020, **7**, 025010.
11. F. Liu, J. Zhou, S. Wang, B. Wang, C. Shen, L. Wang, Q. Hu, Q. Huang and A. Zhou, Preparation of high-purity V₂C MXene and electrochemical properties as Li-ion batteries, *J. Electrochem. Soc.*, 2017, **164**, A709.
12. X. Wang, S. Lin, H. Tong, Y. Huang, P. Tong, B. Zhao, J. Dai, C. Liang, H. Wang and X. Zhu, Two-dimensional V₄C₃ MXene as high-performance electrode materials for supercapacitors, *Electrochim. Acta*, 2019, **307**, 414-421.
13. X. Sang, Y. Xie, D. E. Yilmaz, R. Lotfi, M. Alhabeb, A. Ostadhossein, B. Anasori, W. Sun, X. Li and K. Xiao, In situ atomistic insight into the growth mechanisms of single layer 2D transition metal carbides, *Nat. Commun.*, 2018, **9**, 1-9.
14. L. Ding, L. Li, Y. Liu, Y. Wu, Z. Lu, J. Deng, Y. Wei, J. Caro and H. Wang, Effective ion sieving with Ti₃C₂T_x MXene membranes for the production of drinking water from seawater, *Nat. Sustain.*, 2020, **3**, 296-302.
15. M. Khazaei, M. Arai, T. Sasaki, C. Y. Chung, N. S. Venkataramanan, M. Estili, Y. Sakka and Y. Kawazoe, Novel electronic and magnetic properties of two-dimensional transition metal carbides and nitrides, *Adv. Funct. Mater.*, 2013, **23**, 2185-2192.

16. H. Xiang, H. Lin, L. Yu and Y. Chen, Hypoxia-irrelevant photonic thermodynamic cancer nanomedicine, *ACS Nano*, 2019, **13**, 2223-2235.
17. B. N. Khirak, M. Hasanzadeh, M. Mojaddami, H. S. Far and A. Simchi, In situ synthesis of quasi-needle-like bimetallic organic frameworks on highly porous graphene scaffolds for efficient electrocatalytic water oxidation, *ChemComm* 2020, **56**, 3135-3138.
18. X. Xie, C. Chen, N. Zhang, Z.-R. Tang, J. Jiang and Y.-J. Xu, Microstructure and surface control of MXene films for water purification, *Nat. Sustain.*, 2019, **2**, 856-862.
19. X. Wang, T. S. Mathis, K. Li, Z. Lin, L. Vlcek, T. Torita, N. C. Osti, C. Hatter, P. Urbankowski and A. Sarycheva, Influences from solvents on charge storage in titanium carbide MXenes, *Nature Energy*, 2019, **4**, 241-248.
20. A. VahidMohammadi, J. Rosen and Y. Gogotsi, The world of two-dimensional carbides and nitrides (MXenes), *Science*, 2021, **372**.
21. J. Yang, M. Naguib, M. Ghidui, L. M. Pan, J. Gu, J. Nanda, J. Halim, Y. Gogotsi and M. W. Barsoum, Two-dimensional Nb-based M4C3 solid solutions (MXenes), *J. Am. Ceram. Soc.*, 2016, **99**, 660-666.
22. P. Cai, Q. He, L. Wang, X. Liu, J. Yin, Y. Liu, Y. Huang and Z. Huang, Two-dimensional Nb-based M4C3Tx MXenes and their sodium storage performances, *Ceram. Int.*, 2019, **45**, 5761-5767.
23. Z. Liu, E. Wu, J. Wang, Y. Qian, H. Xiang, X. Li, Q. Jin, G. Sun, X. Chen and J. Wang, Crystal structure and formation mechanism of (Cr₂/3Ti₁/3) 3AlC₂ MAX phase, *Acta Mater.*, 2014, **73**, 186-193.
24. R. Meshkian, Q. Tao, M. Dahlqvist, J. Lu, L. Hultman and J. Rosen, Theoretical stability and materials synthesis of a chemically ordered MAX phase, Mo₂ScAlC₂, and its two-dimensional derivate Mo₂ScC₂ MXene, *Acta Mater.*, 2017, **125**, 476-480.
25. B. Tunca, T. Lapauw, O. M. Karakulina, M. Batuk, T. Cabioc'h, J. Hadermann, R. Delville, K. Lambrinou and J. Vleugels, Synthesis of MAX phases in the Zr-Ti-Al-C system, *Inorg. Chem.*, 2017, **56**, 3489-3498.
26. B. Anasori, M. Dahlqvist, J. Halim, E. J. Moon, J. Lu, B. C. Hosler, E. a. N. Caspi, S. J. May, L. Hultman and P. Eklund, Experimental and theoretical characterization of ordered MAX phases Mo₂TiAlC₂ and Mo₂Ti₂AlC₃, *J.App. Phys.*, 2015, **118**, 094304.
27. Y. Ma, N. Liu, L. Li, X. Hu, Z. Zou, J. Wang, S. Luo and Y. Gao, A highly flexible and sensitive piezoresistive sensor based on MXene with greatly changed interlayer distances, *Nat. Commun.*, 2017, **8**, 1-8.
28. J. Ran, G. Gao, F.-T. Li, T.-Y. Ma, A. Du and S.-Z. Qiao, Ti₃C₂ MXene co-catalyst on metal sulfide photo-absorbers for enhanced visible-light photocatalytic hydrogen production, *Nat. Commun.*, 2017, **8**, 1-10.
29. X. Wang, S. Kajiyama, H. Iinuma, E. Hosono, S. Oro, I. Moriguchi, M. Okubo and A. Yamada, Pseudocapacitance of MXene nanosheets for high-power sodium-ion hybrid capacitors, *Nat. Commun.*, 2015, **6**, 1-6.
30. G. Zuo, Y. Wang, W. L. Teo, A. Xie, Y. Guo, Y. Dai, W. Zhou, D. Jana, Q. Xian and W. Dong, Ultrathin ZnIn₂S₄ nanosheets anchored on Ti₃C₂TX MXene for photocatalytic H₂ evolution, *Angew. Chem., Int. Ed.*, 2020, **59**, 11287-11292.
31. Q. Wan, S. Li and J.-B. Liu, First-principle study of Li-ion storage of functionalized Ti₂C monolayer with vacancies, *ACS Appl. Mater. Interfaces*, 2018, **10**, 6369-6377.
32. R. A. Soomro, S. Jawaid, Q. Zhu, Z. Abbas and B. Xu, A mini-review on MXenes as a versatile substrate for advanced sensors, *Chin. Chem. Lett.*, 2020, **31**, 922-930.
33. L. Qin, J. Jiang, Q. Tao, C. Wang, I. Persson, M. Fahlman, P. O. Persson, L. Hou, J. Rosen and F. Zhang, A flexible semitransparent photovoltaic supercapacitor based on water-processed MXene electrodes, *J. Mater. Chem. A*, 2020, **8**, 5467-5475.
34. M. Naguib, M. Kurtoglu, V. Presser, J. Lu, J. Niu, M. Heon, L. Hultman, Y. Gogotsi and M. W. Barsoum, Two-dimensional nanocrystals produced by exfoliation of Ti₃AlC₂, *Adv.Mater.*, 2011, **23**, 4248-4253.

35. W. Bao, X. Tang, X. Guo, S. Choi, C. Wang, Y. Gogotsi and G. Wang, Porous cryo-dried MXene for efficient capacitive deionization, *Joule*, 2018, **2**, 778-787.
36. K. R. G. Lim, A. D. Handoko, S. K. Nemani, B. Wyatt, H.-Y. Jiang, J. Tang, B. Anasori and Z. W. Seh, Rational design of two-dimensional transition metal carbide/nitride (MXene) hybrids and nanocomposites for catalytic energy storage and conversion, *ACS Nano*, 2020, **14**, 10834-10864.
37. C.-W. Wu, B. Unnikrishnan, I.-W. P. Chen, S. G. Harroun, H.-T. Chang and C.-C. Huang, Excellent oxidation resistive MXene aqueous ink for micro-supercapacitor application, *Energy Storage Mater.*, 2020, **25**, 563-571.
38. Z. Wang, Z. Xu, H. Huang, X. Chu, Y. Xie, D. Xiong, C. Yan, H. Zhao, H. Zhang and W. Yang, Unraveling and regulating self-discharge behavior of Ti₃C₂T_x MXene-based supercapacitors, *ACS Nano*, 2020, **14**, 4916-4924.
39. S. Venkateshalu, J. Cherusseri, M. Karnan, K. S. Kumar, P. Kollu, M. Sathish, J. Thomas, S. K. Jeong and A. N. Grace, New method for the synthesis of 2D vanadium nitride (MXene) and its application as a supercapacitor electrode, *ACS Omega*, 2020, **5**, 17983-17992.
40. L. Xiu, Z. Wang, M. Yu, X. Wu and J. Qiu, Aggregation-resistant 3D MXene-based architecture as an efficient bifunctional electrocatalyst for overall water splitting, *ACS nano*, 2018, **12**, 8017-8028.
41. D. Zhang, S. Wang, R. Hu, J. Gu, Y. Cui, B. Li, W. Chen, C. Liu, J. Shang and S. Yang, Catalytic conversion of polysulfides on single atom zinc implanted MXene toward high-rate lithium-sulfur batteries, *Adv. Funct. Mater.*, 2020, **30**, 2002471.
42. A. Rafieerad, A. Amiri, G. L. Sequiera, W. Yan, Y. Chen, A. A. Polycarpou and S. Dhingra, Development of fluorine-free tantalum carbide Mxene hybrid structure as a biocompatible material for supercapacitor electrodes, *Adv. Funct. Mater.*, 2021, 2100015.
43. C. F. Du, K. N. Dinh, Q. Liang, Y. Zheng, Y. Luo, J. Zhang and Q. Yan, Self-assemble and in situ formation of Ni_{1-x}Fe_xPS₃ nanomosaic-decorated MXene hybrids for overall water splitting, *Adv. Energy Mater.*, 2018, **8**, 1801127.
44. D. Jin, L. R. Johnson, A. S. Raman, X. Ming, Y. Gao, F. Du, Y. Wei, G. Chen, A. Vojvodic and Y. Gogotsi, Computational screening of 2D ordered double transition-metal carbides (MXenes) as electrocatalysts for hydrogen evolution reaction, *J. Phys. Chem. A*, 2020, **124**, 10584-10592.
45. Y. Zhu, K. Rajoua, S. Le Vot, O. Fontaine, P. Simon and F. Favier, Modifications of MXene layers for supercapacitors, *Nano Energy*, 2020, **73**, 104734.
46. P. Forouzandeh and S. C. Pillai, MXenes-based nanocomposites for supercapacitor applications, *Curr. Opin. Chem.*, 2021, **33**, 100710.